

# High efficient As(III) removal by self-assembled zinc oxide micro-tubes synthesized by a simple precipitation process

Weiye Yang · Qi Li · Shian Gao · Jian Ku Shang

Received: 29 January 2011 / Accepted: 5 April 2011 / Published online: 13 April 2011  
© Springer Science+Business Media, LLC 2011

**Abstract** Zinc oxide (ZnO) micro-tubes via self-assembly of nanoparticles were synthesized by a simple precipitation process. Removal of As(III) (arsenite) from water by ZnO micro-tubes through adsorption was investigated with both lab-prepared and natural water samples. The result showed that these self-assembled ZnO micro-tubes are effective to remove As(III) from both lab-prepared and natural water samples at near neutral pH environment. These ZnO micro-tubes have a high adsorption capability on As(III) at low As(III) concentration. When the equilibrium As(III) concentration was around 0.1 mg/L, the amount of As(III) adsorbed at equilibrium was over 10 mg/g. At high equilibrium concentration, the adsorption capacity of these ZnO micro-tubes on As(III) reached over 39.4 mg/g. These ZnO micro-tubes could provide a simple single-step treatment option to treat arsenic-contaminated natural water, which requires no pre-treatment or post-treatment pH adjustment for current industrial practice.

## Introduction

Arsenic contamination in natural water poses a great threat to millions of people in the world [1, 2]. Chronic arsenic

exposure could cause a lot of health problem, such as cancers of liver, lung, kidney, bladder, and skin [3, 4], cardio vascular system problem [5], and the affection on the mental development of children [6]. In 2001, the US Environmental Protection Agency (USEPA) revised the maximum contaminant level (MCL) for arsenic in drinking water from 50 to 10  $\mu\text{g/L}$  and required its compliance since January 2006 [7, 8]. Two major inorganic arsenic species, namely As(III) (arsenite) and As(V) (arsenate), exist in natural water. Among various arsenic removal techniques, adsorption is believed to be a simple and cost-effective process, especially when the arsenic concentration is low as in the natural water environment [9, 10]. Due to the non-ionic existence of As(III) as  $\text{H}_3\text{AsO}_3$  in natural water with pH value ranging from weakly acidic to weakly alkaline, the adsorption performance of various adsorbents on As(III) is usually poor [11–13]. A pre-treatment of oxidizing As(III) to As(V) and/or pH adjustment is necessary for its effective removal from water before coagulation–precipitation or adsorption processes [14–17]. Thus, to simplify the treatment process and lower the treatment cost, it is desirable to develop adsorbents able to effectively remove As(III) without the oxidation/pH adjustment.

Zinc oxide (ZnO) is an extensively investigated metal oxide, and its research history could go back to many decades [18, 19]. Due to its catalytic, electrical, optoelectronic, and photochemical properties, it has been widely utilized in various technical fields as pigments, rubber additives, gas sensors, varistors, semiconductors, optoelectronic devices, and solar cells [19]. Over the past decade, nano/micro-sized ZnO had attracted extensive research attentions. For example, ZnO nanobelts [20] and nanowires [21, 22] had recently been synthesized with unique optical properties. A lot of efforts had been made to develop methods to synthesize ZnO into nano/micro-size

W. Yang · Q. Li (✉) · S. Gao · J. K. Shang  
Materials Center for Water Purification, Shenyang National  
Laboratory for Materials Science, Institute of Metal Research,  
Chinese Academy of Sciences, Shenyang 110016, People's  
Republic of China  
e-mail: qili@imr.ac.cn

J. K. Shang  
Department of Materials Science and Engineering,  
University of Illinois at Urbana-Champaign, Urbana,  
IL 61801, USA

structures with various morphologies [20–33], such as vapor phase transport [20–22], seeded growth process [23], precipitation [24], hydrolysis [25], pyrolysis [26], and hydrothermal process [27, 28].

Herein, we report the synthesis of ZnO micro-tubes self-assembled by ZnO nanoparticles via a simple precipitation process and examined their adsorption effect on As(III) with both lab-prepared and natural water samples at near neutral pH environment. No report is currently available on the systematic study of As(III) adsorption by ZnO in literature [34]. For the first time, a high degree of As(III) removal effect was observed on these ZnO micro-tubes, especially when the As(III) concentration is low as that in most arsenic-contaminated natural water bodies. These ZnO micro-tubes successfully removed the As(III) contamination completely from natural water samples of Lake Yangzonghai with a relatively low material loading. With further development, this technology may offer a simple single-step treatment option to treat arsenic-contaminated natural water without the pre-treatment requirement for current industrial practice.

## Experimental

### Materials system

Zinc acetate dihydrate ( $\text{Zn}(\text{CH}_3\text{COO})_2 \cdot 2\text{H}_2\text{O}$ ,  $\geq 99.0\%$ , Shen Yang Kemiou Chemicals Co. Ltd., Shenyang, P. R. China) and ammonium carbonate ( $(\text{NH}_4)_2\text{CO}_3$ ,  $\text{NH}_3 \geq 40.0\%$ , Sinopharm Chemical Reagent Co., Ltd., Shanghai, P. R. China) were used for the synthesis of hydrozincite ( $\text{Zn}_4\text{CO}_3(\text{OH})_6 \cdot \text{H}_2\text{O}$ ) nanoparticles as received without further purification. Sodium metaarsenite ( $\text{NaAsO}_2$ , Shanghai Tian Ji Chemical Institute, Shanghai, P. R. China) was used to prepare As(III) stock solution, and concentrated hydrochloric acid ( $\text{HCl}$ , 32–38%, Tianda Chemical Reagents Factory, Tianjin, P. R. China) was used to stabilize the arsenic species after treatment. Two commercially available powders were used for the comparison with ZnO micro-tubes on their As(III) removal performance. One is ZnO powder of analytical reagent grade ( $\text{ZnO}$ ,  $\geq 99.0\%$ , Sinopharm Chemical Reagent Co., Ltd., Shanghai, P. R. China). The other one is Degussa P25  $\text{TiO}_2$  nanoparticles (Evonik Industries, Germany), which is commercially available and widely used in the study of arsenic adsorption from water.

### Synthesis of self-assembly ZnO micro-tubes

In a typical synthesis process, 1.756 g  $\text{Zn}(\text{CH}_3\text{COO})_2 \cdot 2\text{H}_2\text{O}$  was dissolved in 10 mL deionized (DI) water to obtain solution 1, and 3.148 g  $(\text{NH}_4)_2\text{CO}_3$  was dissolved in 20 mL

DI water to obtain solution 2. After being stirred magnetically for 30 min, solution 1 was added into solution 2 dropwise at room temperature, and the mixture was kept stirring vigorously during the precipitation process. During this process, the appearance of white precipitates could be observed in the mixture. After being further stirred for 1 h, the white precipitates were collected by centrifugation and washed with DI water repeatedly until neutral pH. The precipitates were then dried at 60–70 °C for a day. The final product was obtained by calcinating the precipitates at 300 °C for 2 h in air.

### Characterization of ZnO micro-tubes

The crystal structures of the precipitates and ZnO micro-tubes were analyzed by the D/MAX-2004-X-ray powder diffractometer (Rigaku Corporation, Tokyo, Japan) with Ni-filtered Cu ( $0.15418 \text{ nm}$ ) radiation at 56 kV and 182 mA. The thermal decomposition of the precipitates was examined by TG–DSC (SETSYS Evolution18, SETARAM Corporation, France) at the rate of 5 °C/min in air. Field emission scanning electron microscopy (FESEM) and transmission electron microscopy (TEM) were utilized to examine their morphology. The SEM images were obtained with a SUPRA35 Field Emission Scanning Electron Microscope (ZEISS, Germany). SEM samples were made by dispersing ZnO micro-tubes in ethanol, applying a drop of the dispersion on a conductive carbon tape, and drying in air for 12 h. Before imaging, the sample was sputtered with gold for 20 s (Emitech K575 Sputter Coater, Emitech Ltd., Ashford Kent, UK). TEM observation was carried out on a JEOL 2010 TEM (JEOL Ltd., Tokyo, Japan) operated at 200 kV, with point-to-point resolution of 0.28 nm. TEM samples were made by dispersing a thin film of ZnO micro-tubes on a Cu grid. BET surface area was measured by  $\text{N}_2$  adsorption/desorption isotherm with an Autosorb-1 Series Surface Area and Pore Size Analyzers (Quantachrome Instruments, Boynton Beach, FL, USA). The zeta-potential curve of ZnO micro-tubes was measured with an electrophoretic spectroscopy (JS84H, Shanghai Zhongchen Digital Instrument Co., Ltd., Shanghai, P. R. China).

### As(III) removal from water samples

A stock solution of 1.333 mM ( $\sim 100 \text{ mg/L}$ ) As(III) was prepared by dissolving  $\text{NaAsO}_2$  into DI water, and stored in the dark in a refrigerator. To investigate the initial As(III) concentration effect, the stock solution was diluted to two initial As(III) concentrations (903.2 and 97.8  $\mu\text{g/L}$ ) for the kinetic study of As(III) adsorption on ZnO micro-tubes. 903.2  $\mu\text{g/L}$  is in the high range of arsenic species concentration found in natural water around the world, and

97.8  $\mu\text{g/L}$  is in the middle to low range [35]. Both As(III) solutions have the pH value of  $\sim 7.0$ , near the neutral state. To investigate the removal effect of ZnO micro-tubes on arsenic-contaminated natural water, natural water samples from Lake Yangzonghai (a major lake in Yunnan Province, P. R. China) were also used in the As(III) removal experiment, in which the As(III) concentration was found at  $\sim 78.1 \mu\text{g/L}$  and its pH value is  $\sim 7.0$ . During the As(III) removal experiment, the arsenic solution was stirred magnetically to disperse ZnO micro-tubes to ensure a good contact between ZnO and arsenic contamination. After recovering the adsorbent by centrifugation, one drop of concentrated HCl was added into the pellucid solution to preserve its arsenic species. The samples were analyzed by an atomic fluorescence spectrophotometer (AFS-9800, Beijing KeChuangHaiGuang Instrument Inc., Beijing, P. R. China) to determine the remaining concentration of As(III).

## Results and discussion

### Characterization of self-assembled ZnO micro-tubes

The X-ray diffraction pattern of the white precipitate is shown in Fig. 1a. It demonstrates that the precipitate obtained by the chemical reaction between  $\text{Zn}(\text{CH}_3\text{COO})_2 \cdot 2\text{H}_2\text{O}$  and  $(\text{NH}_4)_2\text{CO}_3$  is mainly crystallized  $\text{Zn}_4\text{CO}_3(\text{OH})_6 \cdot \text{H}_2\text{O}$ . The TG–DSC curves of the precipitate are shown in Fig. 1b. The TG curve indicates that a remarkable mass loss ( $\sim 23\%$ ) occurred during the precipitate's thermal decomposition, and the DSC curve indicates that it is an endothermic process. The precipitate began to decompose when the temperature was above  $200^\circ\text{C}$ , and the decomposition was complete at  $\sim 270^\circ\text{C}$ . Thus, the calcination temperature used in the synthesis process ( $300^\circ\text{C}$ ) is adequate to obtain pure ZnO final product. Figure 1c shows the X-ray diffraction pattern of the ZnO final product after the calcination. It demonstrates that the hexagonal phase of ZnO was obtained. The average crystallite size of the hexagonal phase is  $\sim 22.5 \text{ nm}$ , obtained by the Scherrer's formula [36]:

$$D = 0.9\lambda / \beta \cos\theta, \quad (1)$$

where  $\lambda$  is the average wavelength of the X-ray radiation,  $\beta$  is the line-width at half-maximum peak position, and  $\theta$  is the diffracting angle.

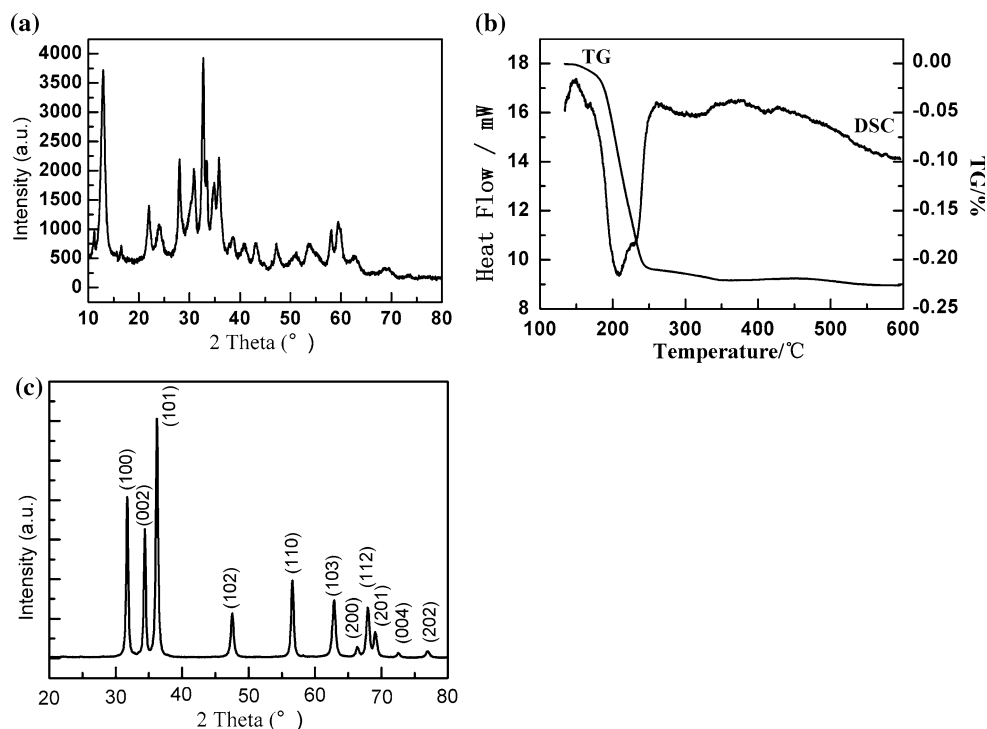
The morphologies of the precipitate ( $\text{Zn}_4\text{CO}_3(\text{OH})_6 \cdot \text{H}_2\text{O}$ ) and ZnO final product were examined with FESEM and TEM. Figure 2a shows the FESEM image of the precipitate, which demonstrated that an interesting micro-tube structure was formed by self-assembly of nano-sized particles during the chemical reaction between  $\text{Zn}(\text{CH}_3\text{COO})_2$  and  $(\text{NH}_4)_2\text{CO}_3$ . Figure 2b and c show the

FESEM images of the ZnO final product with different magnifications. During the calcination process, this interesting micro-tube structure was preserved. The length of these self-assembled ZnO micro-tubes could be over  $10 \mu\text{m}$ , and their diameter is around  $2\text{--}3 \mu\text{m}$  (Fig. 2b). From the high magnification FESEM image (Fig. 2c), it is clear that these micro-tubes were self-assembled by nanoparticles in the range of  $20\text{--}30 \text{ nm}$ , which is very close to the calculated hexagonal phase crystallite size. Figure 2d and e show the HRTEM images of a single self-assembled ZnO micro-tube, which clearly demonstrate that its micro-sized tube structure is self-assembled from large numbers of ZnO nanoparticles ( $\sim 20\text{--}30 \text{ nm}$ ). Nano-sized ZnO had been synthesized into various structures as nanoparticles, nanobelts, nanowires, nanorods, and nanotubes. However, this kind of ZnO micro-tubes self-assembled by nanoparticles is new, and had not yet been reported before.

### Surface properties of self-assembled ZnO micro-tubes

It is well known that there are two major requirements on the adsorbent to obtain the efficient adsorption performance. One is that the adsorbent should possess a large surface area where the adsorption could occur, and the other is that the adsorbent surface should have a good affiliation to the substance that needs to be adsorbed. Figure 3a shows the BET measurement curve of ZnO micro-tubes. The BET-specific surface area of these ZnO micro-tubes was found to be  $51.42 \text{ m}^2/\text{g}$ , which is over 10 times larger than that of AR grade ZnO at  $4.94 \text{ m}^2/\text{g}$  (see Fig. 3b). The pore volume of these ZnO micro-tubes is  $2.67 \times 10^{-1} \text{ cm}^3/\text{g}$ , while the pore volume of AR grade ZnO is only  $7.37 \times 10^{-3} \text{ cm}^3/\text{g}$  ( $\sim 3\%$  of that of these ZnO micro-tubes). Thus, compared with commercially available AR grade ZnO, the much larger surface area and pore volume are beneficial for these ZnO micro-tubes to have better contact efficiency to substances needing to be adsorbed from aqueous environment. The pore size distribution of these ZnO micro-tubes is demonstrated in Fig. 3c. The two peaks at  $\sim 10$  and  $20 \text{ nm}$ , respectively, should reflect the inter-nanoparticle mesoporosity of the tube walls, while the long tail reflects the macropores of the tubes. This observation is in accordance with the morphology of these ZnO micro-tubes as demonstrated in their HRSEM and HRTEM images. Figure 3d shows the zeta potential of these ZnO micro-tubes. Their isoelectric point (IEP) is determined at  $\text{pH} \sim 6.0$ . When the pH value is above 6.0, these ZnO micro-tubes are negatively charged. Thus, at the near neutral aqueous environment (most natural water bodies), hydroxyl groups exist on the surface of these ZnO micro-tubes, which is beneficial for an effective As(III) adsorption as suggested by Pena et al. [35] in their adsorption mechanism study of arsenic on  $\text{TiO}_2$ .

**Fig. 1** **a** X-ray diffraction pattern, **b** TG–DSC curves of the precipitate, and **c** X-ray diffraction pattern of ZnO micro-tubes



#### Kinetic studies on As(III) adsorption by self-assembled ZnO micro-tubes

Batch experiment results of the kinetic studies on As(III) adsorption by ZnO micro-tubes in lab-prepared water samples are shown in Fig. 4. Two initial As(III) concentrations, 97.8 and 903.2  $\mu\text{g/L}$ , were used in the study, which could represent the concentration of As(III) in the low to middle range, and the high range in natural water environment, respectively. When the initial As(III) concentration is 97.8  $\mu\text{g/L}$  (Fig. 4a), it is found that  $\sim 62$ ,  $\sim 93$ , and 100% of As(III) in the water sample could be removed with 0.01, 0.02, and 0.04 g/L ZnO material loadings, respectively. Thus, with just 0.02 g/L ZnO material loading (20 ppm), the equilibrium As(III) concentration in the water sample was less than 7  $\mu\text{g/L}$  after the treatment, which meets the USEPA standard for arsenic in drinking water. This small material loading equals to a volume ratio of adsorbent to treated water at  $3.5:10^6$ , which demonstrates its high adsorption efficiency. When the initial As(III) concentration is 903.2  $\mu\text{g/L}$ ,  $\sim 58$ ,  $\sim 90$ , and 100% of As(III) could be removed with 0.04, 0.08, and 0.10 g/L ZnO material loadings, respectively. Even for such a high As(III) concentration, ZnO micro-tubes demonstrated an excellent removal effect. When the ZnO micro-tubes loading concentration was just 0.1 g/L,  $\sim 80\%$  As(III) in the solution was removed in just 30 min, and 100% As(III) could be removed after the treatment. Thus, a single-step high efficient As(III) removal process is practical with these ZnO micro-tubes, which requires no

pre-treatment (oxidation and pH adjustment) and post-treatment pH adjustment.

The kinetic study results could be best fitted into a pseudo-second-order rate kinetic model as demonstrated in Fig. 4c and d. A pseudo-second-order rate expression [37] is defined by Eq. 2 and its integrated form is given in Eq. 3:

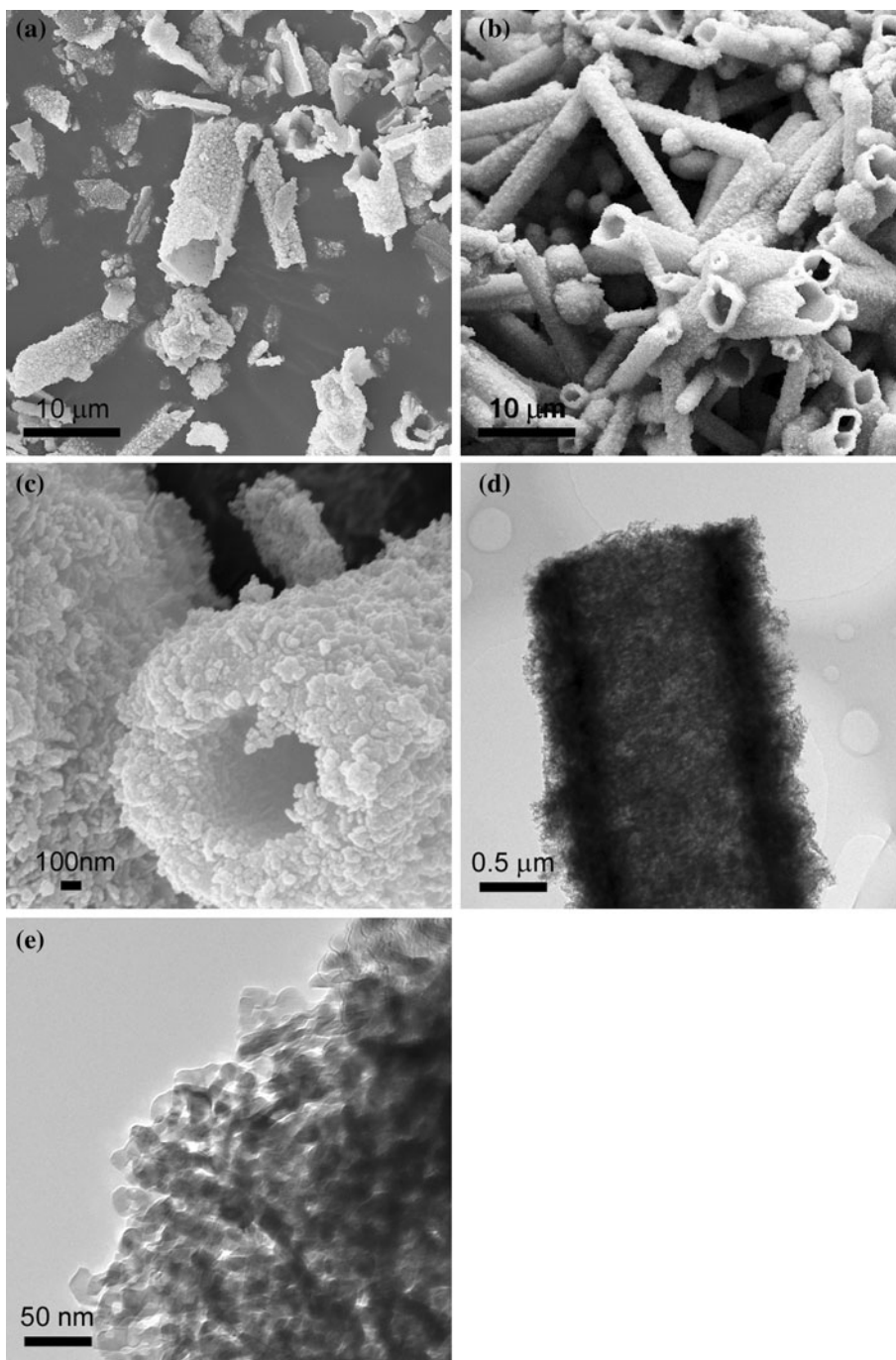
$$dq_t/dt = K_{ad}(q_e - q_t)^2 \quad (2)$$

$$t/q_t = 1/(K_{ad}q_e^2) + t/q_e, \quad (3)$$

where  $q_e$  and  $q_t$  are the capacities ( $\text{mg g}^{-1}$ ) of arsenic adsorbed at equilibrium and at time  $t$ , respectively, and  $K_{ad}$  is the rate constant of adsorption ( $\text{mg g}^{-1} \text{min}^{-1}$ ). The kinetic parameters obtained in fitting the experimental data are summarized in Table 1. The applicability of the pseudo-second-order rate model was quantified by the square of the correlation coefficient  $R$  ( $R^2$ ), and the closeness of  $R^2$  to 1 indicates that the model fitted the experimental data accurately. With the increase of adsorbent to As(III) ratio, the ratio of the amount of As(III) adsorbed at equilibrium to the initial amount of arsenic increases, and the rate constant ( $K_{ad}$ ) also improves indicating a faster adsorption of As(III).

Due to the various differences in the experimental conditions, it is not possible to directly compare the adsorption efficiency among reports in literature. In Ref. [17], Meng and co-workers synthesized a nanocrystalline  $\text{TiO}_2$  with a large specific surface area of  $330 \text{ m}^2/\text{g}$ . In their study, the initial As(III) solution concentration is 2.0  $\text{mg/L}$ , the pH value is 7.0, and the amount of  $\text{TiO}_2$  is 0.2 g/L. The

**Fig. 2** **a** FESEM image of the precipitate, **b** and **c** FESEM images of ZnO micro-tubes, **d** and **e** HRTEM images of ZnO micro-tubes



reported adsorption  $K_{ad}$  is  $0.199 \mu\text{mol}^{-1} \text{g h}^{-1}$ , which equals to  $0.015 \text{mg}^{-1} \text{g h}^{-1}$ . With even smaller powder to arsenic species ratio (about 88.6%) in our experiment (initial As(III) concentration at  $0.9032 \text{mg/L}$ , pH value at 7.0, and the amount of ZnO at  $0.08 \text{g/L}$ ), the  $K_{ad}$  is determined at  $0.3 \text{mg}^{-1} \text{g h}^{-1}$ , about 20 times of their reported value. When the material loading of ZnO increases to  $0.1 \text{g/L}$ , which provides a powder to arsenic species ratio about 10% higher than that used in their experiment, the  $K_{ad}$  is determined to be  $0.9 \text{mg}^{-1} \text{g h}^{-1}$ , about 60 times of their reported value. These ZnO micro-tubes have a

much smaller surface area (about one-sixth) compared with their  $\text{TiO}_2$  nanoparticles. Thus, these comparisons demonstrate that these ZnO micro-tubes possess a very good affiliation to As(III).

#### Equilibrium adsorption isotherm study on As(III) adsorption by ZnO micro-tubes

The equilibrium adsorption isotherm study was conducted to investigate the adsorption capacity of these ZnO micro-tubes on As(III) at near neutral pH environment. Because

**Fig. 3** **a** BET curve of ZnO micro-tubes, **b** BET surface areas and pore volumes of ZnO micro-tubes and AR grade ZnO powder, **c** pore size distribution, and **d** zeta-potential measurement of ZnO micro-tubes

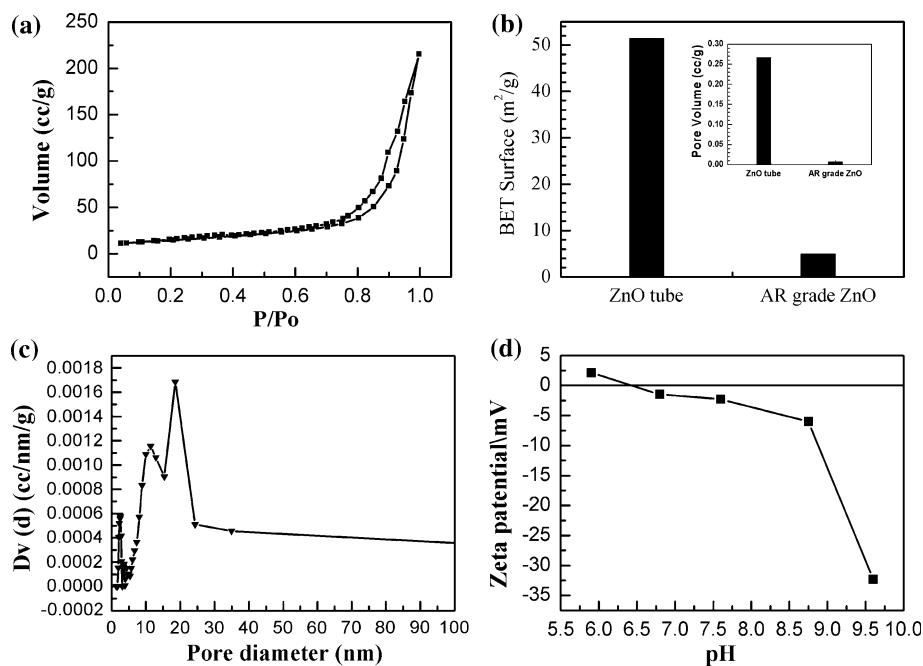


**Fig. 4** Adsorption kinetics of As(III) on ZnO micro-tubes: **a** initial As(III) concentration is  $\sim 97.8 \mu\text{g/L}$  and **b** initial As(III) concentration is  $\sim 903.2 \mu\text{g/L}$ . **c** and **d** The pseudo-second-order rate kinetic model fitting of the adsorption kinetics studies demonstrated in **a** and **b**, respectively

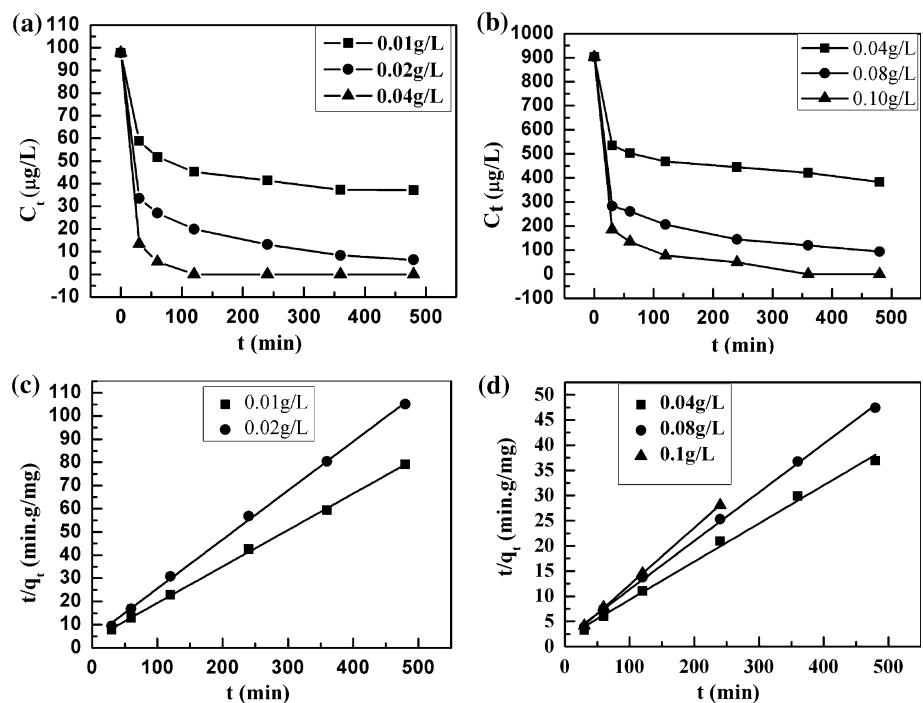


**Table 1** Kinetic parameters for As(III) adsorption onto ZnO micro-tubes

Initial As(III) concentration (mg/L)	0.0978	0.9032			
Materials loading (g/L)	0.01	0.02	0.04	0.08	0.1
$q_e$ (mg g <sup>-1</sup> )	6.360	4.731	13.193	10.367	8.805
$K_{ad}$ (mg <sup>-1</sup> g min <sup>-1</sup> )	0.007	0.010	0.003	0.005	0.015
$R^2$	0.999	0.999	0.995	0.999	0.999

the concentration of As(III) in contaminated natural water bodies is usually low, equilibrium adsorption isotherm under low equilibrium As(III) concentration was also investigated, besides of the commonly demonstrated equilibrium adsorption isotherm under high equilibrium As(III) concentration. The parameters obtained in fitting the experimental data are summarized in Table 2. Figure 5a demonstrates the equilibrium adsorption isotherm when the equilibrium As(III) concentration was from

**Table 2** Equilibrium adsorption isotherm fitting parameters for As(III) onto ZnO micro-tubes

Equilibrium As(III) concentration upper limit (mg/L)	113	
Freundlich isotherm	$K_F$	13.779
	$n$	4.579
	$R^2$	0.976

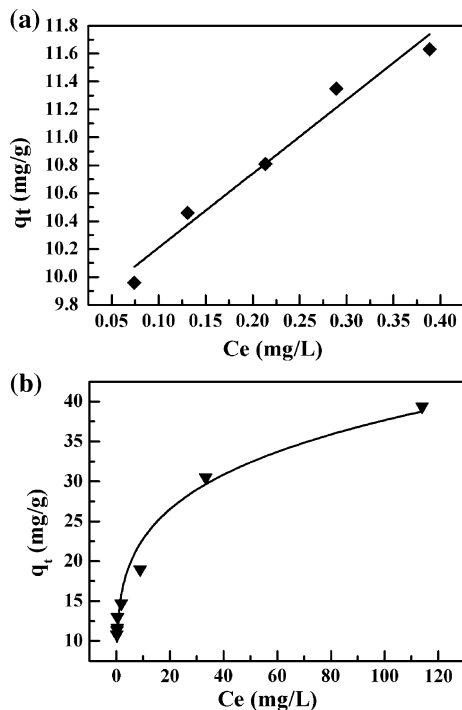


**Fig. 5** The equilibrium adsorption isotherm of As(III) on ZnO micro-tubes: **a** the equilibrium As(III) concentration was low (up to 0.4 mg/L) and **b** the equilibrium As(III) concentration was high (up to 113 mg/L)

0.07 to 0.4 mg/L. Under such a low equilibrium As(III) concentration, the amount of As(III) adsorbed at equilibrium follows a linear relationship with the equilibrium As(III) concentration. When the equilibrium As(III) concentration is around 0.1 mg/L, the amount of As(III) adsorbed at equilibrium could be over 10 mg/g, which indicates that these ZnO micro-tubes could possess a high As(III) removal efficiency from contaminated natural water bodies usually with low As(III) concentrations.

Figure 5b demonstrates the equilibrium adsorption isotherm when the equilibrium As(III) concentration was high (up to 110 mg/L). The adsorption data could be best fitted with the Freundlich isotherm as given in Eq. 4:

$$q_e = K_F \times c_e^{1/n}, \tag{4}$$

where  $q_e$  is the amount (mg g<sup>-1</sup>) of As(III) adsorbed at equilibrium,  $c_e$  is the equilibrium As(III) concentration

(mg/L) in water samples, and  $K_F$  and  $n$  are the adsorption constants. Figure 5b shows the adsorption capability of these ZnO micro-tubes on As(III) is no less than 39.4 mg/g, and it could further increase with the increase of the equilibrium As(III) concentration.

As(III) removal performance compared with AR grade ZnO powders and Degussa P25 TiO<sub>2</sub> nanoparticles

Obvious differences on As(III) adsorption performance were observed between ZnO micro-tubes, AR grade ZnO powders, and Degussa P25 TiO<sub>2</sub> nanoparticles (Fig. 6a). With the same material loading of 0.04 g/L, AR grade ZnO powders and Degussa P25 TiO<sub>2</sub> nanoparticles could only remove about 60 and 50% As(III) in the water sample after 8 h treatment, respectively. ZnO micro-tubes, however, could remove As(III) from the water sample completely to meet the USEPA standard for arsenic in drinking water within just 2 h. The enhanced As(III) adsorption performance of ZnO micro-tubes may be attributed to their larger surface area, higher pore volume, and very good affiliation to As(III).

As(III) removal on natural water samples from Lake Yangzonghai by ZnO micro-tubes

To examine the removal effect of these ZnO micro-tubes in the natural water environment, kinetic studies of their As(III) adsorption performance on natural water samples from Lake Yangzonghai was conducted, which was recently contaminated by arsenic from industrial pollution. Figure 6b shows the decrease of As(III) concentration in the water sample from Lake Yangzonghai with the increase of the treatment time. These ZnO micro-tubes also demonstrated a good adsorption performance on As(III) in the natural water sample, although there might be competition effect from other species in natural water. With only a low material loading of 0.06 g/L (60 ppm), the As(III) concentration in this contaminated lake water sample dropped to ~10 μg/L in 30 min, and further dropped to zero within 4 h. Thus, these ZnO micro-tubes are capable to remove As(III) in natural water bodies to meet the USEPA standard for arsenic in drinking water.

**Conclusions**

The ZnO with an interesting micro-tube structure was synthesized by a simple precipitation process, and its As(III) removal effect from water was investigated in both lab-prepared and natural water samples. ZnO micro-tubes demonstrated an effective As(III) removal performance on both lab-prepared and natural water samples. The amount of As(III) adsorbed at equilibrium could be over 10 mg/g at

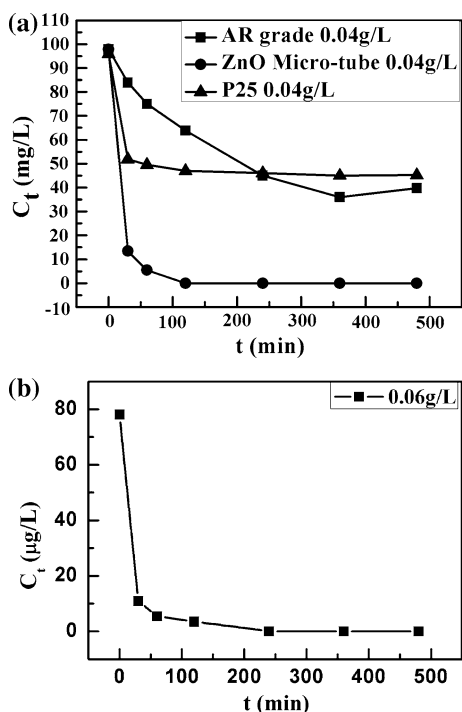


**Fig. 6** **a** The decrease of As(III) concentration in lab-prepared samples with the increase of the treatment time by ZnO micro-tubes, AR grade ZnO powder, and Degussa P25 TiO<sub>2</sub> nanoparticles at 0.04 g/L material loading. **b** The decrease of As(III) concentration in natural water samples from Lake Yangzonghai with the increase of the treatment time at 0.06 g/L ZnO micro-tubes

near neutral pH environment when the equilibrium As(III) concentration is around 0.1 mg/L, which indicates that these ZnO micro-tubes could possess a high As(III) removal efficiency from contaminated natural water bodies usually with low As(III) concentrations. With only a relatively low material loading of 0.06 g/L, these ZnO micro-tubes successfully removed the As(III) contamination completely from natural water samples of Lake Yangzonghai. Thus, these ZnO micro-tubes could provide a simple single-step treatment option to treat arsenic-contaminated natural water, which requires no pre-treatment or post-treatment pH adjustment and could lower the cost and the pollution risk from adding large amount of chemicals into natural water bodies. The desorption of adsorbed As(III) on ZnO micro-tubes could be easily achieved by their interaction with weak alkaline solution. These ZnO micro-tubes could then be recycled to reduce the operation cost, and arsenic in the enriched weak alkaline solution could be extracted by standard industry practices for various applications.

**Acknowledgements** This study was supported by the National Basic Research Program of China, Grant No. 2006CB601201, the Knowledge Innovation Program of Chinese Academy of Sciences,

Grant No. Y0N5711171, and the Knowledge Innovation Program of Institute of Metal Research, Grant No. Y0N5A111A1.

## References

- Nordstrom D (2002) *Science* 296(5576):2143
- Amini M, Abbaspour K, Berg M, Winkel L, Hug S, Hoehn E, Yang H, Johnson C (2008) *Environ Sci Technol* 42(10):3669
- Smith A, Lingas E, Rahman M (2000) *Bull World Health Organ* 78:1093
- Hopenhayn-Rich C, Biggs M, Smith A (1998) *Int J Epidemiol* 27(4):561
- Xia Y, Liu J (2004) *Toxicology* 198(1–3):25
- Saha K (2003) *Crit Rev Environ Sci Technol* 33(2):127
- Smith A, Lopipero P, Bates M, Steinmaus C (2002) *Science* 296(5576):2145
- US EPA (2000) Technologies and costs for removal of arsenic from drinking water. US Environmental Protection Agency, Washington
- Mohan D, Pittman C (2007) *J Hazard Mater* 142(1–2):1
- Zhang G, Qu J, Liu H, Liu R, Li G (2007) *Environ Sci Technol* 41(13):4613
- Borho M, Wilderer P (1996) *Water Sci Technol* 34(9):25
- Lee H, Choi W (2002) *Environ Sci Technol* 36(17):3872
- Kim Y, Kim C, Choi I, Rengaraj S, Yi J (2004) *Environ Sci Technol* 38(3):924
- Edwards M (1994) *J Am Water Works Assoc* 86(9):64
- McNeill L, Edwards M (1995) *J Am Water Works Assoc* 87(4):105
- Hering J (1996) *J Am Water Works Assoc* 88(4):155
- Pande S, Deshpande L, Patni P, Lutade S (1997) *J Environ Sci Health Part A* 32(7):1981
- Özgür Ü, Alivov Y, Liu C, Teke A, Reshchikov M, Doğan S, Avrutin V, Cho S, Morkoc H (2005) *J Appl Phys* 98:041301
- Meyer B, Alves H, Hofmann A, Kriegseis W, Forster D, Bertram F, Christen J, Hoffmann A, Straburg M, Dworzak M (2004) *Phys Status Solidi (b)* 241(2):231
- Pan Z, Dai Z, Wang Z (2001) *Science* 291(5510):1947
- Huang M, Mao S, Feick H, Yan H, Wu Y, Kind H, Weber E, Russo R, Yang P (2001) *Science* 292(5523):1897
- Yang P, Yan H, Mao S, Russo R, Johnson J, Saykally R, Morris N, Pham J, He R, Choi H (2002) *Adv Funct Mater* 12(5):323
- Tian Z, Voigt J, Liu J, Mckenzie B, Mcdermott M, Rodriguez M, Konishi H, Xu H (2003) *Nat Mater* 2(12):821
- Iwasaki M, Inubushi Y, Ito S (1997) *J Mater Sci Lett* 16(18):1503
- Jézéquel D, Guenot J, Jouini N, Fiévet F (1995) *J Mater Res* 10(1):77
- Milosevic O, Uskokovic D (1993) *Mater Sci Eng A* 168(2):249
- Chen D, Jiao X, Cheng G (1999) *Solid State Commun* 113(6):363
- Li W, Shi E, Tian M, Zhong W (1998) *Sci China Ser E Technol Sci* 41(5):449
- Zhang J, Sun L, Yin J, Su H, Liao C, Yan C (2002) *Chem Mater* 14(10):4172
- Yao B, Chan Y, Wang N (2002) *Appl Phys Lett* 81:757
- Yamabi S, Imai H (2002) *J Mater Chem* 12(12):3773
- Hu J, Bando Y (2003) *Appl Phys Lett* 82:1401
- Li Q, Kumar V, Li Y, Zhang H, Marks T, Chang R (2005) *Chem Mater* 17(5):1001
- Hristovski K, Baumgardner A, Westerhoff P (2007) *J Hazard Mater* 147(1–2):265
- Pena M, Korfiatis G, Patel M, Lippincott L, Meng X (2005) *Water Res* 39(11):2327
- Barrett C, Massalski TB (1966) *Structure of metals*. McGraw Hill, New York
- Sa Y, Aktay Y (2002) *Biochem Eng J* 12(2):143